Bull. Mater. Sci., Vol. 32, No. 1, February 2009, pp. 103–107. © Indian Academy of Sciences.

X-ray absorption spectroscopy of $PbMoO_4$ single crystals

D BHATTACHARYYA[†], A K POSWAL[†], S N JHA[†], SANGEETA and S C SABHARWAL*
Crystal Technology Laboratory, TPPED, [†]Spectroscopy Division, Bhabha Atomic Research Centre, Mumbai 400 085, India

MS received 25 April 2008

Abstract. **X-ray absorption spectra of $PbMoO_4$ (LMO) crystals have been investigated for the first time in literature. The measurements have been carried out at Mo absorption edge at the dispersive EXAFS beamline (BL-8) of INDUS-2 Synchrotron facility at Indore, India. The optics of the beamline was set to obtain a band of 2000 eV at 20,000 eV and the channels of the CCD detector were calibrated by recording the absorption edges of standard Mo and Nb foils in the same setting. The absorption spectra have been measured for three LMO samples prepared under different conditions viz. (i) grown in air from stoichiometric starting charge, (ii) grown in argon from stoichiometric starting charge and (iii) grown in air from PbO-rich starting charge. The results have been explained on the basis of the defect structure analysed in LMO crystals prepared under different conditions. The Mo absorption edge is significantly influenced by the deviations in crystal stoichiometry.**

Keywords. **$PbMoO_4$ crystal; Mo foil; X-ray absorption spectroscopy; synchrotron radiation.**

1. Introduction

$PbMoO_4$ (LMO) crystals have long been exploited for commercial applications in acoustic–optic modulators (Bonne and Zydik 1970; Zeng 1997). However, several fundamental aspects pertaining to crystal growth and characterization still remain unexplored. LMO crystals are generally grown from a polycrystalline LMO precursor obtained by mixing the two constituent oxides viz. PbO and MoO_3, taken in desired proportion and raising it to the melting temperature. A major problem faced with the growth of LMO crystals is the occurrence of non-stoichiometry, which arises due to the excessive vapour pressure of MoO_3 over PbO at elevated temperatures. The preferential and uncontrolled depletion of MoO_3 during growth gives rise to colouration and cracking of the as-grown crystals (Zeng 1996; Bochkova *et al* 2003; Sabharwal *et al* 2006; Sangeeta *et al* 2006; Tyagi *et al* 2008). The presence of defects arising as a consequence of the stoichiometric deviations is also found to influence the crystal ionic conductivity (Neiman *et al* 1984).

The influence of inert ambient provided during growth which causes non-stoichiometry in the oxygen sub-lattice has also been investigated. It is observed (Sabharwal *et al* 2006; Sangeeta *et al* 2006) that crack-free and transparent crystals can be obtained by performing the growth in air from a slightly Mo-excess starting charge. Optical transmission study shows that the highest optical transmission is achieved with such crystals. It has further been observed that crystals grown from a slightly Pb excess precursor in air or those grown from a stoichiometric precursor in argon ambient show the development of an absorption band over the wavelength range of 400–500 nm.

X-ray diffraction (XRD) results show that a doublet structure is developed in (312) and (224) reflections corresponding to d values of 1·653 Å and 1·622 Å, respectively for crystals grown using stoichiometric precursors in argon ambient or Pb-excess precursors under normal ambient (Sangeeta *et al* 2006). Whereas, in crystals grown from Mo-excess precursors in air the doublet structure is found to be absent. X-ray photoelectron spectroscopy (XPS) results revealed that the Mo 3d spectrum, which consists of a single peak for crystals grown from stoichiometric precursors in air, splits into a doublet when the growth is carried out under argon atmosphere (Sangeeta *et al* 2006). These results show that the constituent atomic species in LMO may attain different valence states, depending on crystal stoichiometry. To further investigate this aspect, X-ray absorption spectra of the LMO crystals near the Mo absorption edge have been studied. It may be mentioned that this is the first ever report of X-ray absorption measurement of LMO crystals employing synchrotron radiation.

2. Experimental

The samples for X-ray absorption spectroscopy were prepared from single crystal pieces of $PbMoO_4$ (LMO)

*Author for correspondence (sudhirsabharwal@yahoo.co.in)

grown by Czochralski technique (Sabharwal *et al* 2006; Sangeeta *et al* 2006). The three samples prepared for the present investigation were (a) grown from a stoichiometric charge in air, (b) from a stoichiometric charge in argon and (c) grown in air from a starting charge containing 1% excess PbO. In the subsequent text these three samples have been identified as LMO-1, LMO-2 and LMO-3, respectively. The crystal pieces were finely powdered and mixed homogenously with a suitable low Z material and self-supporting pellets were prepared using a hydraulic press.

2.1 *Computation of sample concentration for absorption measurements*

The absorption coefficient (μ) for a compound material is given by

$$\mu = \left[\sum_i \left(\frac{\mu}{\rho}\right)_i g_i\right]\rho = \left[\sum_i (\mu_m)_i g_i\right]\rho, \quad (1)$$

where $(\mu_m)_i$ is the mass absorption coefficient and g_i the molar concentration of the ith element of the compound and ρ the density of the compound. For a cylindrical pellet of such a compound having surface area, A and thickness, t, the total absorption is given by

$$\mu t = \left[\sum_i \left(\frac{\mu}{\rho}\right)_i g_i\right]\rho t, \quad (2)$$

whereas, the weight of the compound is given by

$$W = At\rho. \quad (3)$$

From (2) and (3) the weight to surface ratio is computed as

$$\frac{W}{A} = \frac{\mu t}{\sum_i \left(\frac{\mu}{\rho}\right)_i g_i}. \quad (4)$$

Table 1 gives the mass absorption coefficients of Pb, Mo and O at energies of 19,980 eV and 20,020 eV, i.e. at values just below and above the Mo absorption edge at 20,000 eV as obtained from the XAID data base available within the X-ray Oriented Programming (XOP) package (Sanchez del Rio and Dejus 1998). In order to obtain a value of total absorption $(\mu t)_H$ above Mo absorption edge equal to ~4·0, W/A should be equal to ~0·06 g cm^{-2}. The corresponding value of total absorption $(\mu t)_L$ below Mo absorption edge comes out to be ~2·95. This data yields an edge jump, $(\Delta\mu = \mu t_H - \mu t_L) \sim 1{\cdot}05$, which should be easily detectable in X-ray absorption measurements. Thus, for the present experiment, 75 mg of $PbMoO_4$ was mixed with ~3·5 g of cellulose acetate and pellets of 12 mm diameter and 3 mm thick were prepared which yielded an effective surface density (W/A) of ~0·066 g cm^{-2}.

Table 1. Mass absorption coefficients of Pb, Mo and O below and above the MoK-edge absorption.

	Mass absorption coefficient at different photon energies (μ_m)(cm^2 g^{-1})	
Element	19,980 eV	20,020 eV
Pb	83·0	83·0
Mo	12·0	80·0
O	0·60	0·60

2.2 *Configurational details of EXAFS set up*

The X-ray absorption measurements were performed at the recently developed BL-8 Dispersive EXAFS beamline at 2·5 GeV INDUS-2 Synchrotron Source at RRCAT, Indore, India. A schematic diagram describing the basic principle of the beam line is shown in figure 1. The beamline uses a single crystal (CC), which can be bent to take shape of an ellipse such that the source (S_0) and the sample positions (S_3) are situated at the two foci of an ellipse (Lee *et al* 1994). White synchrotron radiation emerging from the source (S_0) is dispersed and focussed at the sample (S_3) by the bent crystal. The radiation transmitted through the sample is detected by a position-sensitive CCD detector (D). The whole absorption spectrum can thus be recorded simultaneously in a short duration of ~300 ms. A bent Si (111) crystal having 2d value equal to 6·2709 Å is used to cover the photon energy range of 5000–20,000 eV and provides bandwidths of 300 eV, 1000 eV and 2000 eV, respectively at photon energies of 5000 eV, 10,000 eV and 20,000 eV.

The present measurements were carried out in transmission mode at MoK edge of 20,000 eV by appropriately setting the crystal bender at 20,000 eV position so that a bandwidth of 2000 eV is obtained on the CCD detector. The absorption edges of standard Mo and Nb foils were recorded to calibrate the CCD channels. The plot of sample absorption versus photon energy was obtained by recording the CCD output with (I) and without (I_0) samples and using the relation, $I = I_0 e^{-\mu t}$.

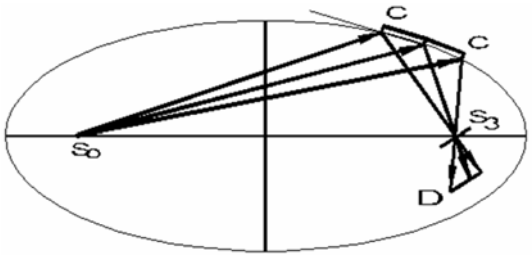

Figure 1. Schematic showing the working principle of the dispersive EXAFS beamline (BL-8) at INDUS-2 Synchrotron facility, Indore, India. Where, S_0 is the synchrotron source, CC the crystal, S_3 the sample under investigation and D the detector.

3. Results and discussion

Figure 2 shows the absorption spectra of 99·99% pure Nb and Mo foils (M/s Goodfellow) recorded at the same setting of the crystal bender and the CCD detector. The absorption edges of Nb and Mo are found to appear at CCD channel numbers of 1577 and 1067, respectively. From the known values of the Nb and Mo K-edges at 18,986 eV and 20,000 eV, respectively (X-ray Data booklet), the CCD channels are calibrated w.r.t. energy. The absorption spectrum of a MoO_3 pellet pressed using 99·9% pure powder (M/s Sigma-Aldrich) together with that of Mo foil is shown in figure 3. A clear shift in absorption edges of MoO_3 and elemental Mo is clearly seen from the figure. The absorption spectra of the above two samples near the absorption edges have been fitted using the ATHENA code available within the IFEFFIT package (Newville *et al* 1995) and the exact edge positions at the half edge steps have been derived for both the samples. The edge positions in figure 3 show an edge shift of ~9·34 eV between elemental Mo and MoO_3. This agrees well with the results reported in literature (Lutzenkrichen-Hecht and Frahm 1999), thus showing good resolution of the present experimental set up.

In the same setting of the crystal bender, the absorption edges of the three $PbMoO_4$ samples were recorded and the plots obtained are shown in figure 4. The signature of Mo absorption edge is clearly seen in samples prepared in air from a stoichiometric precursor (LMO-1). However, the absorption jump is observed to be more prominent in crystals grown from stoichiometric precursors under argon atmosphere (LMO-2). Of course, the absorption edge is considerably flat in this case. It is seen that LMO-3, which

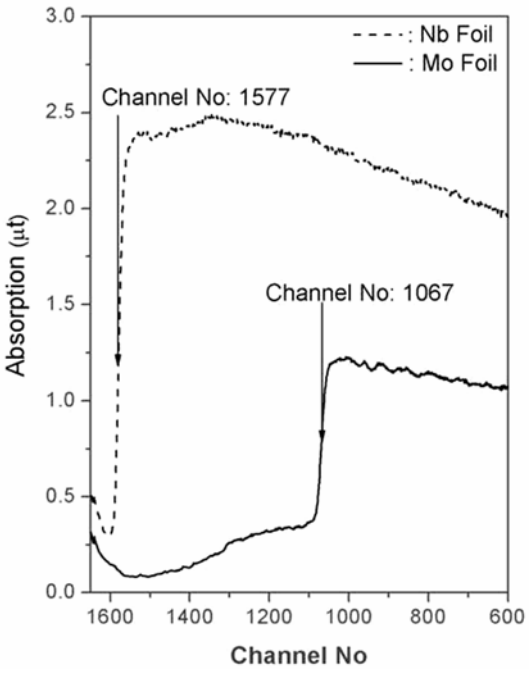

Figure 2. X-ray absorption spectra of Nb and Mo foils in the same setting of the crystal bender and detector.

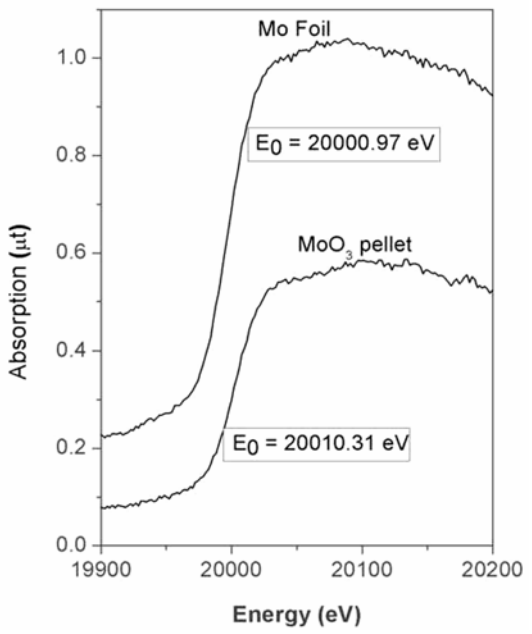

Figure 3. X-ray absorption spectra of Mo foil and polycrystalline MoO_3 around 20,000 eV.

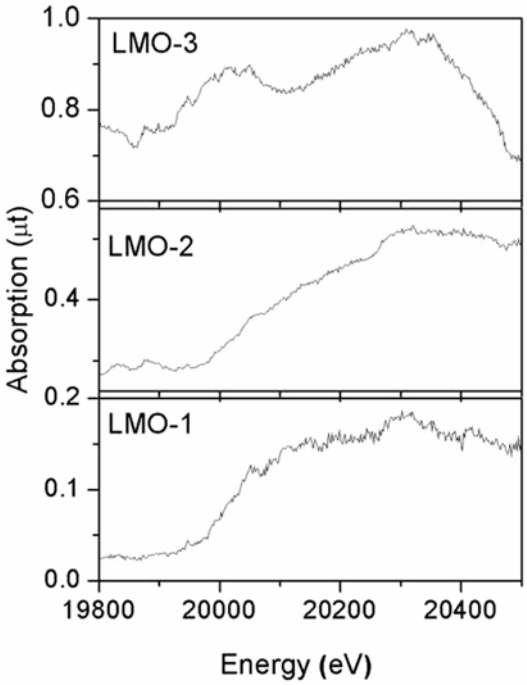

Figure 4. X-ray absorption spectra of $PbMoO_4$ crystals grown under different conditions: (i) stoichiometric grown in air (LMO-1), (ii) stoichiometric grown in argon (LMO-2) and (iii) grown in air from a starting charge containing 1% excess PbO (LMO-3).

Table 2. Possible lattice disorders present in LMO crystals grown under different conditions.

Crystal identification	Starting charge	Growth ambient	Lattice disorders
LMO-1	Constituent powders mixed in the stoichiometric ratio	Air	Mo-vacancies, Mo vacancies occupied by Pb^{+4} ions
LMO-2	Constituent powders mixed in the stoichiometric ratio	Argon	Presence of Mo ions in different electronic states due to non-stoichiometry developed in anionic sublattice
LMO-3	PbO rich	Air	Excess Pb^{+2} ions in interstitial position, Pb^{+4} ions at Mo vacancy sites

is grown from a PbO excess starting charge, is characterized by high absorption throughout the energy range and the absence of any clear signature of Mo absorption edge at 20,000 eV. In order to understand these results, we first discuss below the possible scenarios of lattice disorders in LMO crystals prepared under different conditions.

As already mentioned, LMO crystals may be deficient in MoO_3 and hence they would be expected to have the presence of Mo vacancies. In the case of crystals grown from a stoichiometric charge in air, Mo vacancy may be occupied by a Pb ion stabilizing in +4 state because of the matching of the ionic radii of Pb^{+4} (0·76 Å) and Mo^{+6} (0·65 Å) ions. Under this situation, the crystal lattice would contain Pb ions stabilized in two different electronic states. The observations by Bochkova *et al* (2003) and Bollmann (1980) that the yellow colouration in LMO crystals grown from a stoichiometric charge is due to the acceptor defects is in conformity with this model. Also, the model is supported by the observations of Neiman *et al* (1984) that the ionic character of electrical conductivity in colourless LMO crystals (absence of Mo vacancies) changes to electronic in coloured crystals (presence of Pb^{+4} ions).

The oxidation of Pb^{+2} to Pb^{+4} state would be suppressed when the crystal growth is carried out in argon atmosphere. In this case the Mo vacancies, if present in the lattice, cannot be occupied by Pb^{+2} ions due to a large mismatch between the ionic radii of Pb^{+2} (1·20 Å) and Mo^{+6} (0·65 Å) ions. Here, the non-stoichiometry is promoted in the oxygen sub-lattice, which necessitates stabilization of some of the Mo ions in lower valence state. This model is supported by the X-ray photoelectron spectroscopy (XPS) results of Sangeeta *et al* (2006), which shows the presence of both Mo^{+5} and Mo^{+6} ions in LMO-2 crystals.

The crystals grown from a PbO-rich starting charge (LMO-3) would have a significant amount of Pb at the interstitial sites because the loss of PbO from the melt due to evapouration is very small at the operating temperatures (Sangeeta and Sabharwal 2008). Besides, some of the Pb^{+4} ions at the Mo vacancy site would also be present in LMO-3.

The different situations visualized above have been summarized in table 2. In the light of the defect structure analysed in LMO, the observed X-ray absorption results are explained as follows. The excess Pb in the case of LMO-3 causes an overall increase in crystal absorption due to large absorption coefficient of Pb on either side of the Mo absorption edge at 20,000 eV. Consequently, the absorption jump at the Mo edge is smeared out in figure 4. The presence of a large number of Pb^{+4} ions at Mo sites is also thought to be responsible for the reduced edge jump in LMO-1. In case of LMO-2 since the non-stoichiometry is introduced in anion sub-lattice and hence a higher absorption jump at Mo edge as expected is indeed observed.

4. Conclusions

The X-ray absorption spectra of $PbMoO_4$ crystals grown from starting charges of different compositions or ambient have been reported for the first time in literature. The measurements were performed using the dispersive EXAFS beam line (BL-8) set up at INDUS-2 Synchrotron facility at Indore, India. The absorption edge jump at Mo absorption edge at 20,000 eV is most significantly visible in case of the crystals grown from a stoichiometric charge under argon atmosphere. The absorption edge is, however, flat which is attributed to the presence of Mo ions stabilizing in more than one oxidation states in the crystal lattice. The absorption jump is small in case of the LMO crystals grown in air from a stoichiometric charge in which case a significant occupancy of Pb^{+4} ions at Mo sites is envisaged. The LMO crystals grown from a Pb excess charge shows high absorption over the whole spectral range and hence the absence of a clear edge jump at Mo absorption edge. The results have been discussed in the light of the possible lattice disorders present in LMO crystals grown under different conditions. The most significant outcome of the current investigation is the effect of crystal non-stoichiometry on Mo absorption edge. Further, EXAFS investigations are required to shine light on crystal defect structure.

Acknowledgements

Authors are grateful to Dr Anil Kakodkar, Chairman AEC, Dr Srikumar Banerjee, Director, BARC and Dr V C

Sahni, Director, RRCAT, for their valuable guidance, support and encouragement to set up the EXAFS beamline at INDUS-2, RRCAT, Indore.

References

Bochkova T M, Volnyanskii M D, Volnyanskii D M and Shchetinkin V S 2003 *Phys. Solid State* **45** 244

Bollmann W 1980 *Kristall und Technik* **15** 367, 585

Bonne W A and Zydik G J 1970 *J. Cryst. Growth* **7** 65

Lee P L, Beno M A, Jennings G, Ramanathan M, Knapp G S, Huang K, Bai J and Montano P A 1994 *Rev. Sci. Instrum.* **65** 1

Lutzenkrichen-Hecht D and Frahm R 1999 *J. Synch. Rad.* **6** 591

Neiman A Y, Afanasiev A A, Feodorova L M, Gabrielian V T and Karagezian S M 1984 *Phys. Status Solidi (a)* **83** 153

Newville M, Ravel B, Haskel D, Rehr J J, Stern E A and Yacoby Y 1995 *Physica* **B208 & 209** 154

Sabharwal S C, Sangeeta and Desai D G 2006 *Cryst. Growth and Design* **6** 58

Sanchez del Rio M and Dejus R J 1998 *SPIE* **2448** 340 (http://www.esrf.fr/computing/scientific/xop)

Sangeeta, Desai D G, Singh A K, Tyagi M and Sabharwal S C 2006 *J. Cryst. Growth* **296** 81

Sangeeta and Sabharwal S C 2008 *J. Cryst. Growth* (doi:10.1016/j.jcrysgro.2008.01.048)

Tyagi M, Sangeeta, Desai D G and Sabharwal S C 2008 *J. Luminesc.* **128** 22

X-ray Data booklet 2001 Lawrence Berkeley National Laboratory, University of California, Berkeley

Zeng H C 1996 *J. Mater. Res.* **11** 703

Zeng H C 1997 *J. Cryst. Growth* **171** 136